FEBS Letters 588 (2014) 3862–3869

journal homepage: www.FEBSLetters.org

Hrr25 phosphorylates the autophagic receptor Atg34 to promote vacuolar transport of α-mannosidase under nitrogen starvation conditions

Keisuke Mochida [a], Yoshinori Ohsumi [b], Hitoshi Nakatogawa [a,b,*]

[a] Graduate School of Bioscience and Biotechnology, Tokyo Institute of Technology, Japan
[b] Frontier Research Center, Tokyo Institute of Technology, Japan

ARTICLE INFO

Article history:
Received 5 September 2014
Revised 17 September 2014
Accepted 17 September 2014
Available online 2 October 2014

Edited by Noboru Mizushima

Keywords:
Selective autophagy
Autophagosome
Nitrogen starvation
Yeast
Casein kinase 1
Vacuolar enzyme

ABSTRACT

In *Saccharomyces cerevisiae*, under nitrogen-starvation conditions, the α-mannosidase Ams1 is recognized by the autophagic receptor Atg34 and transported into the vacuole, where it functions as an active enzyme. In this study, we identified Hrr25 as the kinase that phosphorylates Atg34 under these conditions. Hrr25-mediated phosphorylation does not affect the interaction of Atg34 with Ams1, but instead promotes Atg34 binding to the adaptor protein Atg11, which recruits the autophagy machinery to the Ams1–Atg34 complex, resulting in activation of the vacuolar transport of Ams1. Our findings reveal the regulatory mechanism of a biosynthetic pathway mediated by the autophagy machinery.

Structured summary of protein interactions:
Hrr25 phosphorylates **Atg34** by protein kinase assay (View interaction)
Ams1 and **Atg34** colocalize by fluorescence microscopy (View interaction)
Atg34 physically interacts with **Ams1** by anti tag coimmunoprecipitation (View interaction)
Atg11 physically interacts with **Atg34** by cross-linking study (View interaction)

1. Introduction

Autophagy is a lysosomal or vacuolar degradation pathway in which various cytoplasmic components are selectively or non-selectively sequestered by double-membrane vesicle autophagosomes and transported into the lytic compartments [1–3]. This process requires a unique set of proteins called autophagy-related (Atg) proteins, which play central roles in forming the autophagosomal membrane and determining cargo selectivity. The autophagy machinery is also utilized to transport enzymes that function in the vacuole. In the cytoplasm-to-vacuole targeting (Cvt) pathway of the budding yeast *Saccharomyces cerevisiae*, three vacuolar enzymes, the aminopeptidases Ape1 and Ape4 and the α-mannosidase Ams1, are recognized by the receptor protein Atg19, and these proteins form an aggregate-like structure called the Ape1 complex [4–8]. Atg19 also interacts with the adaptor protein Atg11. Atg11 targets the Ape1 complex to the vacuole and recruits the Atg proteins that mediate the formation of the autophagosomal membrane, which sequesters the Ape1 complex [7]. When the vesicle formed fuses with the vacuole, the Ape1 complex is released into the vacuolar lumen, where the complex is disassembled and the enzymes begin to function.

S. cerevisiae has a homolog of Atg19, Atg34, which also interacts with Atg11. Whereas Atg19 directly binds all three Cvt cargos, Atg34 specifically recognizes Ams1 [8–10]. A previous study revealed that Atg34 is not involved in the Cvt pathway, but instead serves as a receptor for Ams1 and is involved in its autophagic transport under nitrogen-starvation conditions [9]. That study also showed that Atg34 is phosphorylated under these conditions. This modification might regulate the function of Atg34, but to date the identity of the responsible kinase and how it affects Atg34 function have remained unknown. Here, we show that the casein kinase 1 homolog Hrr25 is the kinase that phosphorylates Atg34 under nitrogen-starvation conditions. Our data suggest that phosphorylation by Hrr25 promotes Atg34 interaction with Atg11 and thereby upregulates the initiation of Ams1 sequestration by the autophagosomal membrane.

* Corresponding author at: Graduate School of Bioscience and Biotechnology, Tokyo Institute of Technology, Yokohama 226-8503, Japan. Fax: +81 45 924 5121.
E-mail address: hnakatogawa@bio.titech.ac.jp (H. Nakatogawa).

http://dx.doi.org/10.1016/j.febslet.2014.09.032
0014-5793/

2. Materials and methods

2.1. Yeast strains and plasmids

The yeast strains and oligonucleotides used in this study are listed in Tables 1 and 2, respectively. Gene tagging and disruption were performed by a PCR-based method [11–13]. pFA6a-*EGFP-kanMX6*, pFA6a-*EGFP-hphNT1*, pFA6a-*mCherry-kanMX6*, pFA6a-*zeoNT3*, pFA6a-*CgHIS3*, and pFA6a-*CgTRP1* (donated by Dr. Hayashi Yamamoto) were used for protein tagging with EGFP and mCherry and for gene disruption with the cassettes of the zeocin-resistant gene, *CgHIS3*, and *CgTRP1*. Cells expressing *ATG34* under the control of the *CET1* promoter were constructed by integrating a DNA fragment containing the *CET1* promoter, which was obtained by PCR using the plasmid pFA6a-*kanMX6-pCET1-VN* [14] and the oligonucleotides CET1pro-ATG34-Fw and -Rv, into the upstream of the start codon of chromosomal *ATG34*. Cells expressing GFP-tagged Atg34 mutants were constructed as follows. The coding sequence of *ATG34* was amplified by PCR using the primers HindIII-ATG34-Fw and ATG34-HindIII-Rv and ligated into the *Hin*dIII site of pFA6a-*EGFP-kanMX6*, resulting in pFA6a-*ATG34–EGFP-kanMX6*. Site-directed mutagenesis was performed using Quick Change kit (Agilent Technologies) for the Ala replacement of Ser382 or Ser383 of Atg34 encoded in this plasmid. DNA fragments obtained by PCR using these plasmids and the primers ATG34-ORF-Fw and ATG34-Ctag-Rv were introduced into yeast cells to replace chromosomal *ATG34* with *ATG34–EGFP-kanMX6* containing the *ATG34* mutations or not by homologous recombination. Cells expressing non-tagged Atg34 mutants were constructed as follows. A DNA fragment encompassing the *ATG34* open reading frame and the promoter region was obtained by PCR using the primers XbaI-ATG34pro-Fw and ATG34-XhoI-Rv and cloned into the *Xba*I-*Xho*I site of the pRS303 vector, and the *ATG34* mutations were introduced into this plasmid by site-directed mutagenesis. DNA fragments encompassing *HIS3* and *ATG34* were amplified by PCR using these plasmids and the primers HIS3pro-Fw and MCS-HIS3-ter-Rv and integrated into the chromosomal *HIS3* locus by homologous recombination in *atg34*Δ cells.

Table 2
Oligonucleotides used in this study.

Name	Sequence
CET1pro-ATG34-Fw	gaaactagttcctataggttgagtgtctatcaaaaatttacggagacgcg GAATTCGAGCTCGTTTAAAC
CET1pro-ATG34-Rv	tgatcgatgacaaagaagtcgaatagtgtcgtttctaccgcaattttcat AGTGGGAGGATAGAAATGCTAC
HindIII-ATG34-Fw	aaaAAGCTTatgaaaattgcggtagaaac
ATG34-HindIII-Rv	aaaAAGCTTtatttcttcccaagtaaatggc
ATG34-ORF-Fw	CTCTAAAATCTCCACTAGCC
ATG34-Ctag-Rv	ttaaataagtactatagccaaagaaactggaagaatataaaaaagcat TTAATCGATGAATTCGAGCTCG
XbaI-ATG34pro-Fw	aaaTCTAGAtcgatcaagaaattaaatga
ATG34-XhoI-Rv	aaaCTCGAGggaagaatataaaaaagcat
HIS3pro-Fw	CGTTTTAAGAGCTTGGTGAG
MCS-HIS3ter-Rv	tccatctcttttatatttttttctcgagttcaagagaaaaaaaaagaaa CTAAAGGGAACAAAAGCTGG

2.2. Media and growth conditions

Yeast cells were grown in YPD medium (1% yeast extract, 2% peptone, and 2% glucose) at 30 °C. To knock down Hrr25 using the auxin-inducible degron (AID) system, indole-3-acetic acid (IAA) in ethanol was added to a final concentration of 0.5 mM, and the same volume of ethanol was added to control samples [13]. Autophagy was induced by addition of 200 ng/ml rapamycin. For fluorescence microscopy, yeast cells grown to mid-log phase in YPD medium were shifted to SD + CA + ATU medium (0.17% yeast nitrogen base without amino acids and ammonium sulfate, 0.5% ammonium sulfate, 0.5% casamino acid, 0.002% adenine sulfate, 0.002% tryptophan, 0.002% uracil, and 2% glucose) containing 200 ng/ml rapamycin and 0.5 mM IAA and incubated for the indicated time periods.

Table 1
Yeast strains used in this study.

Name	Genotype	Figures	Reference
SEY6210	*MATα leu2-3,112 ura3-52 his3-Δ200 trp1-Δ901 suc2-Δ9 lys2-801; GAL*	–	[35]
YKM381	SEY6210 *ura3-52::ADH1pro-OsTIR1–9Myc-URA3*	1A	This study
YKM386	SEY6210 *ura3-52::ADH1pro-OsTIR1–9Myc-URA3 hrr25–aid-natNT2*	1A	This study
YKM409	YKM381 *atg19Δ::zeoNT3 ATG34–EGFP-kanMX6*	2B	This study
YKM410	YKM386 *atg19Δ::zeoNT3 ATG34–EGFP-kanMX6*	2B	This study
YKM424	YKM409 *atg1Δ::hphNT1*	1B, 2B and 3C	This study
YKM425	YKM410 *atg1Δ::hphNT1*	1B and 3C	This study
YKM422	YKM381 *atg19Δ::zeoNT3 atg1Δ::hphNT1*	3C	This study
YKM423	YKM386 *atg19Δ::zeoNT3 atg1Δ::hphNT1*	3C	This study
YKM620	YKM422 *kanMX6-CET1pro-ATG34*	1D	This study
YKM621	YKM423 *kanMX6-CET1pro-ATG34*	1D	This study
YKM578	YKM381 *atg19Δ atg34Δ::CgTRP1*	1D and 4E	This study
YKM405	YKM381 *atg19Δ::zeoNT3 AMS1–EGFP-kanMX6*	2A and 3A	This study
YKM406	YKM386 *atg19Δ::zeoNT3 AMS1–EGFP-kanMX6*	2A and 3A	This study
YKM417	YKM405 *atg34Δ::natNT2*	2A	This study
YKM443	YKM381 *atg19Δ::zeoNT3 atg1Δ::CgHIS3 AMS1–mCherry-kanMX6 ATG34–EGFP-hphNT1*	3B	This study
YKM444	YKM386 *atg19Δ::zeoNT3 atg1Δ::CgHIS3 AMS1–mCherry-kanMX6 ATG34–EGFP-hphNT1*	3B	This study
YKM441	YKM381 *atg19Δ::zeoNT3 atg1Δ::CgHIS3 AMS1–mCherry-kanMX6 ATG11–EGFP-hphNT1*	4B	This study
YKM442	YKM386 *atg19Δ::zeoNT3 atg1Δ::CgHIS3 AMS1–mCherry-kanMX6 ATG11–EGFP-hphNT1*	4B	This study
YKM480	YKM381 *atg19Δ::zeoNT3 pep4Δ::kanMX4*	4A	This study
YKM544	YKM480 *hphNT1-ADH1pro-yeGFP–ATG11*	4A	This study
YKM545	YKM386 *atg19Δ::zeoNT3 pep4Δ::kanMX4 hphNT1-ADH1pro-yeGFP–ATG11*	4A	This study
YKM557	YKM381 *atg19Δ atg34Δ::natNT2 pep4Δ::kanMX4 hphNT1-ADH1pro–yeGFP-ATG11*	4A	This study
YKM631	YKM381 *atg19Δ::zeoNT3 ATG34–EGFP-kanMX6*	4D	This study
YKM632	YKM381 *atg19Δ::zeoNT3 ATG34^{S382A}–EGFP-kanMX6*	4D	This study
YKM633	YKM381 *atg19Δ::zeoNT3 ATG34^{S383A}–EGFP-kanMX6*	4D	This study
YKM561	YKM405 *atg1Δ::hphNT1 atg34Δ::natNT2 his3-Δ200::HIS3-ATG34*	4E	This study
YKM562	YKM405 *atg1Δ::hphNT1 atg34Δ::natNT2 his3-Δ200::HIS3-ATG34^{S383A}*	4E	This study
YKM563	YKM406 *atg1Δ::hphNT1 atg34Δ::natNT2 his3-Δ200::HIS3-ATG34*	4E	This study

2.3. Immunoblotting

Yeast cells harvested by centrifugation were treated with 20% trichloroacetic acid on ice for 20 min, and then centrifuged at 15 000*g* for 5 min. The pellets were washed with cold acetone, dried at room temperature, and suspended in SDS sample buffer, followed by cell disruption using a FastPrep-24 (MP Biomedicals) and 0.5-mm YZB zirconia beads (Yasui Kikai). The samples were boiled and subjected to immunoblotting analysis [15]. To analyze phosphorylation of Atg34 expressed from the *CET1* promoter, cells grown to mid-log phase were spheroplasted, incubated in 0.5× YPD medium containing 1.0 M sorbitol and 0.5 mM IAA for the indicated time periods in the presence or absence of 200 ng/ml rapamycin, and lysed in IP buffer [50 mM Tris-HCl (pH 8.0), 150 mM NaCl, 5 mM EDTA, 5 mM EGTA, 50 mM NaF, and 10% glycerol] containing 0.5% Triton-X100, 2 mM phenylmethylsulfonyl fluoride (PMSF), 2× Complete protease inhibitor cocktail (Roche), 1× PhosSTOP phosphatase inhibitor cocktail (Roche), and 500 nM microcystin. The lysates were centrifuged at 17 400*g* for 20 min, and the supernatants were analyzed by immunoblotting. Antibodies against AID (BioROIS), Pgk1 (Invitrogen), GFP (Roche, 118144 60001), GST (Santa Cruz Biotechnology, B-14), Atg34 [9], and Ams1 [16] were used for the detection of the proteins. The biotinylated Phos-tag (Wako) was used in combination with Streptavidin-HRP (Invitrogen) to detect protein phosphorylation.

2.4. Protein purification

Escherichia coli BL21 cells harboring pGEX-6P-Atg34 (donated by Dr. Nobuo Noda), -Hrr25, or Hrr25 K38A [17], or the pGEX-6P-1 (empty) vector, were cultured at 37 °C in LB media (10 mg/ml tryptone, 5 mg/ml yeast extract, 10 mg/ml NaCl, and 1 mM NaOH) containing 50 μg/ml ampicillin. To induce protein expression, isopropyl β-D-thiogalactopyranoside was added to a final concentration of 0.1 mM. These cells were further cultured at 16 °C for 24 h, harvested, and disrupted in buffer A [20 mM HEPES-KOH (pH 7.2) and 150 mM NaCl] containing 5 mM dithiothreitol (DTT), 0.5 mM EDTA, and 0.1 mM PMSF, as described previously [18]. The GST-tagged proteins were purified using Glutathione Sepharose 4B (GE Healthcare), followed by elution with 50 mM Tris-HCl (pH 8.0) containing 150 mM NaCl and 10 mM reduced glutathione. The GST–Hrr25-bound resins were treated with the PreScission protease (GE Healthcare) to elute Hrr25 without the GST tag. The purified proteins were appropriately concentrated using Vivaspin columns (Sartorius) and stored at −80 °C in solutions containing 25% glycerol.

2.5. In vitro kinase assay

GST or GST–Atg34 (0.3 μM) was incubated at 30 °C with wild-type Hrr25 or Hrr25 K38A (0.05 μM) in 20 mM HEPES-KOH (pH 7.2) containing 150 mM NaCl, 1 mM $MgCl_2$, 0.2 mM DTT, and 1 mM ATP.

2.6. Fluorescence microscopy

Fluorescence microscopy was performed using an inverted fluorescence microscope (Olympus, IX81) equipped with an electron-multiplying CCD camera (Hamamatsu Photonics, ImagEM C9100-13) and a 150× objective lens (Olympus, UAPON

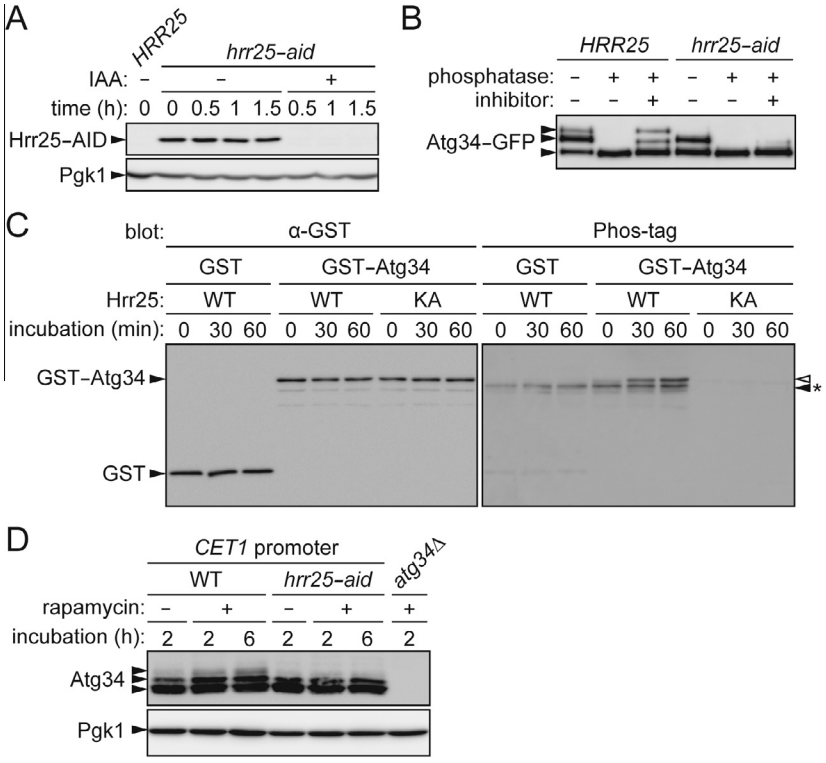

Fig. 1. Hrr25 is the kinase responsible for Atg34 phosphorylation in rapamycin-treated cells. (A) Control (*HRR25*) and *hrr25–aid* cells grown to mid-log phase were treated with or without IAA for the indicated time periods, and then analyzed by immunoblotting using antibodies against AID and Pgk1. Pgk1 serves as a loading control. (B) *HRR25 atg19Δ atg1Δ* and *hrr25–aid atg19Δ atg1Δ* cells expressing Atg34–GFP were grown to mid-log phase and treated with IAA and rapamycin for 6 h. Atg34–GFP was immunoprecipitated using anti-GFP antibody and treated with lambda protein phosphatase in the presence or absence of phosphatase inhibitors, followed by immunoblotting using anti-GFP antibodies. (C) Recombinant GST or GST–Atg34 was incubated with wild-type Hrr25 (WT) or the K38A mutant (KA) in the presence of ATP, and then analyzed by immunoblotting using anti-GST antibody or Phos-tag staining. The white arrowhead represents phosphorylated GST–Atg34. The asterisk indicates the band that probably represents autophosphorylated Hrr25. (D) *HRR25 atg19Δ atg1Δ* and *hrr25–aid atg19Δ atg1Δ* cells were spheroplasted and treated with IAA for the indicated time periods in the presence or absence of rapamycin. These cells were examined by immunoblotting using antibodies against Atg34 and Pgk1.

150XOTIRF, NA/1.45). GFP and mCherry were excited using a 488-nm blue laser (50 mW, Coherent) and a 561-nm yellow laser (50 mW, Coherent), respectively. Fluorescence was filtered with a Di01-R488/561-25 dichroic mirror (Semrock) and an Em01-R488/568-25 bandpass filter (Semrock), and separated into two channels using a U-SIP splitter (Olympus) equipped with a DM565HQ dichroic mirror (Olympus). The fluorescence was further filtered using an FF02-525/50-25 bandpass filter (Semrock) for the GFP channel and an FF01-624/40-25 bandpass filter (Semrock) for the mCherry channel. Images were acquired using the MetaMorph software (Molecular Devices) and processed using MetaMorph and Adobe Photoshop CS6.

2.7. Immunoprecipitation

To examine the Atg34–Ams1 interaction, yeast cells expressing Atg34–GFP were treated with rapamycin for 6 h and disrupted in IP buffer containing 2 mM PMSF, 2× Complete protease inhibitor cocktail (Roche), 1× PhosSTOP phosphatase inhibitor cocktail (Roche), and 500 nM microcystin using a Multi-beads Shocker (Yasui Kikai) and 0.5-mm YZB zirconia beads. The lysates were solubilized at 4 °C for 30 min with 0.2% Nonidet P-40, and then centrifuged at 17 400*g* for 15 min; the supernatants were mixed with GFP-Trap_M beads (ChromoTek) using a rotator at 4 °C for 2 h. After the beads were washed with IP buffer, the bound proteins were eluted by incubating the beads in SDS sample buffer at 65 °C for 10 min. To examine the Atg34–Atg11 interaction, cells expressing GFP–Atg11 under the control of the *ADH1* promoter were spheroplasted by incubation at 30 °C for 1 h in 0.5× YPD containing 1 M sorbitol and 0.2 mg/ml zymolyase 100T (Seikagaku Biobusiness). After washing with HEPES-KOH (pH 7.2) containing 1.2 M sorbitol, the spheroplasts were incubated in 0.5× YPD containing 1.0 M sorbitol and 0.5 mM IAA for 30 min at 30 °C, and then treated with rapamycin for 1 h. For the crosslinking reaction, the spheroplasts were harvested by centrifugation and resuspended in HEPES-KOH (pH 7.2) containing 1.2 M sorbitol and 200 μg/ml DSP (Thermo Scientific), and then incubated at room temperature for 30 min. These spheroplasts were washed with IP buffer containing 1.2 M sorbitol to quench and remove unreacted DSP, and then lysed at 4 °C for 30 min in IP buffer containing 0.5% Triton X-100, 2 mM PMSF, 2× protease inhibitor cocktail, 1× phosphatase inhibitor cocktail, and 500 nM microcystin. The lysates were centrifuged at 17 400*g* for 15 min, and the supernatants were subjected to immunoprecipitation using GFP-Trap_M beads as described above.

2.8. Phosphatase treatment

Immunoprecipitates were obtained using Atg34–GFP-expressing cells and GFP-Trap_M beads as described above. The beads were washed with IP buffer, and then incubated with lambda protein phosphatase (New England Biolabs) at 30 °C for 1 h under the recommended conditions in the presence or absence of 5× Halt phosphatase inhibitor cocktail (Pierce).

3. Results and discussion

3.1. Hrr25 phosphorylates Atg34 under nitrogen-starvation conditions

A previous study showed that Atg34 is phosphorylated under nitrogen-deprived conditions, but did not identify the responsible kinase [9]. We noted that a global analysis of yeast kinase interactions identified Atg34 as a protein that coisolated with the multifunctional kinase Hrr25 [19–24]. This observation prompted us to investigate whether Hrr25 is involved in phosphorylation of Atg34. Because Hrr25 is essential for yeast growth, we took advantage of the auxin-inducible degron (AID) system to knock down its expression [13]. In this system, a target protein tagged with the AID is coexpressed in yeast cells with the plant F-box protein OsTIR1. When these cells are treated with an auxin, the tagged protein is degraded by the ubiquitin–proteasome system. We engineered the genomic *HRR25* gene to express a protein C-terminally tagged with the AID (*hrr25–aid*), and confirmed that Hrr25–AID was efficiently and immediately depleted upon treatment with the auxin indole-3-acetic acid (IAA) (Fig. 1A). Using this system, we examined phosphorylation of Atg34 under Hrr25-depleted conditions. In control cells (*HRR25*) treated with rapamycin, which mimics a nitrogen starvation signal by inactivating the TORC1 complex [25], Atg34–GFP was detected as three bands in immunoblotting analysis (Fig. 1B). Upon lambda protein phosphatase treatment, the top and middle bands were shifted down to converge with the bottom band, suggesting that these two bands represent phosphorylated forms of Atg34. We did not observe the top band in *hrr25–aid* cells treated with IAA. These results suggest that Hrr25 is indeed involved in phosphorylation of Atg34 under nitrogen-deprived conditions. The middle band, which was insensitive to Hrr25 depletion, may indicate Atg34 phosphorylation by another kinase. Alternatively, the band might reflect incomplete depletion of Hrr25; consistent with this idea, *hrr25–aid* cells continued to grow at a slow rate even in the presence of IAA [17].

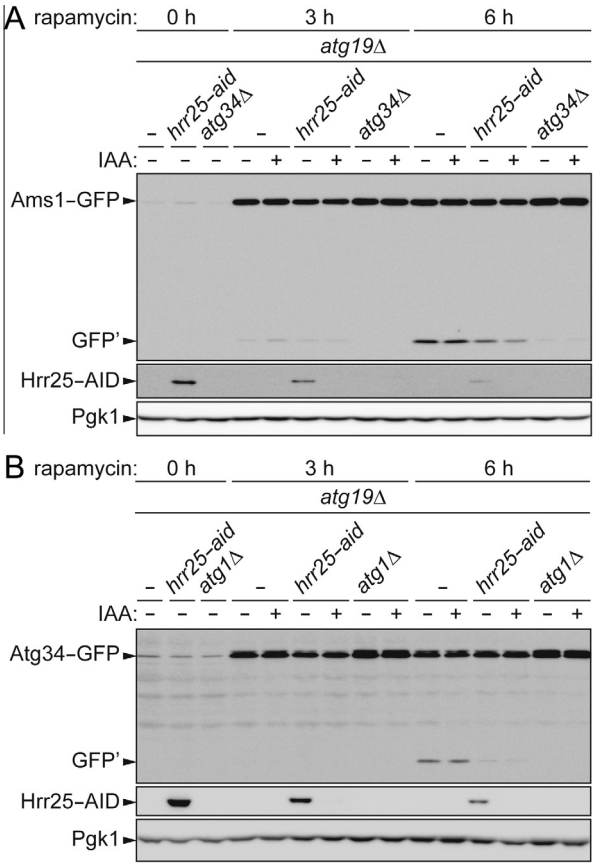

Fig. 2. Vacuolar transport of Ams1 and Atg34 in Hrr25-depleted cells. (A) Yeast cells expressing Ams1–GFP were grown to mid-log phase, treated with or without IAA for 30 min, and then treated with rapamycin for 3 or 6 h. These cells were examined by immunoblotting using antibodies against GFP, AID, and Pgk1. GFP′ represents GFP fragments produced by the vacuolar cleavage of Ams1–GFP. (B) Yeast cells expressing Atg34–GFP were treated with IAA and rapamycin, followed by immunoblotting as described in (A). The vacuolar transport of Atg34–GFP results in the production of GFP fragments (GFP′).

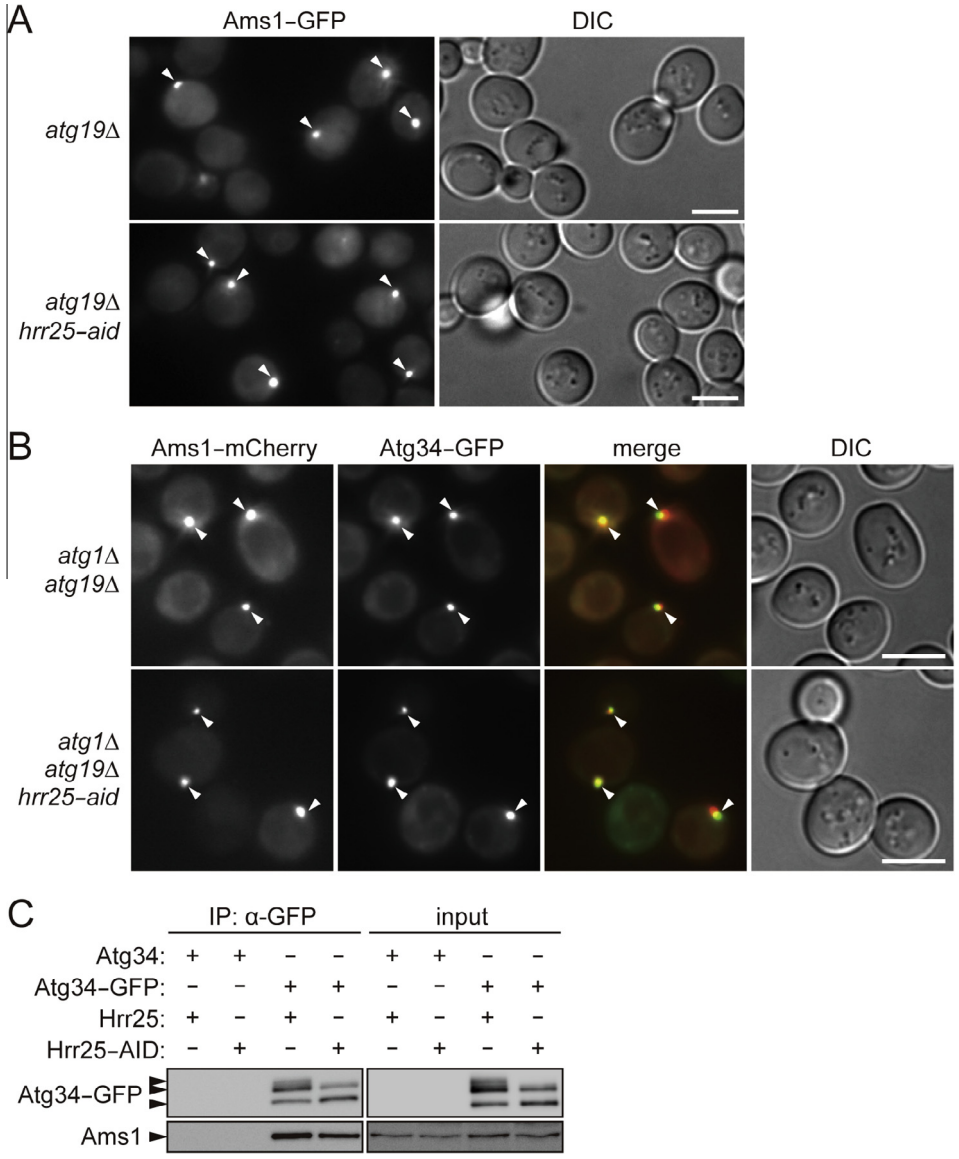

Fig. 3. Ams1 complex assembly occurs normally in Hrr25-depleted cells. (A) Yeast cells expressing Ams1–GFP were treated with rapamycin for 2 h in the presence of IAA and observed under a fluorescence microscope. The arrowheads indicate Ams1–GFP dots that represent the Ams1 complex. DIC, differential interference contrast. Scale bars, 5 μm. (B) Yeast cells coexpressing Ams1–mCherry and Atg34–GFP were treated with rapamycin for 4 h in the presence of IAA, and then analyzed by fluorescence microscopy as described in (A). The arrowheads indicate Ams1–mCherry dots colocalized with Atg34–GFP. Scale bars, 5 μm. (C) Yeast cells lacking Atg19 and Atg1 were treated with IAA and rapamycin for 6 h, and then used to generate whole-cell lysates (input). Immunoprecipitation was performed using anti-GFP antibody, and the precipitates (IP) were analyzed by immunoblotting with antibodies against GFP and Ams1.

We also performed in vitro phosphorylation reactions using recombinant Atg34 and Hrr25, which were expressed in and purified from *E. coli* cells. In these experiments, either GST-fused Atg34 or GST alone was incubated with Hrr25 in the presence of ATP. Phosphorylated proteins were detected using the phosphate-binding reagent Phos-tag following SDS–PAGE separation. When GST–Atg34 was incubated with wild-type Hrr25, the level of Phos-tag–stained GST–Atg34 increased in a time-dependent manner (Fig. 1C). This staining was not observed with the kinase-inactive K38A mutant of Hrr25 [20,26], and Hrr25 did not phosphorylate GST alone. These results suggest that Hrr25 directly phosphorylates Atg34.

We examined whether Atg34 phosphorylation by Hrr25 is constitutive or regulated. Since the expression of Atg34 is largely suppressed under normal conditions [9] (also see Fig. 2B), phosphorylation of the protein under these conditions could not be examined properly. Thus, we replaced the promoter of chromosomal *ATG34* with that of constitutively expressing *CET1*. Using this strain, we showed that Hrr25-mediated phosphorylation of Atg34 is promoted by rapamycin treatment (Fig. 1D), suggesting that this modification is involved in the stimulation of the autophagic transport of Ams1 by nitrogen starvation.

3.2. Hrr25 is required for Atg34-dependent vacuolar transport of Ams1 under nitrogen-starvation conditions

Next, we asked whether Hrr25 is required for the Atg34-mediated autophagic transport of Ams1. Because two autophagic receptors, Atg19 and Atg34, function redundantly in Ams1 transport under nitrogen-depleted conditions, we disrupted *ATG19* to examine the function of Atg34 [9]. Vacuolar transport of Ams1 was monitored by detecting GFP fragments (GFP′) generated by the cleavage of Ams1–GFP in the vacuole [9]. As reported previously, *atg19Δ* cells accumulated GFP fragments when treated

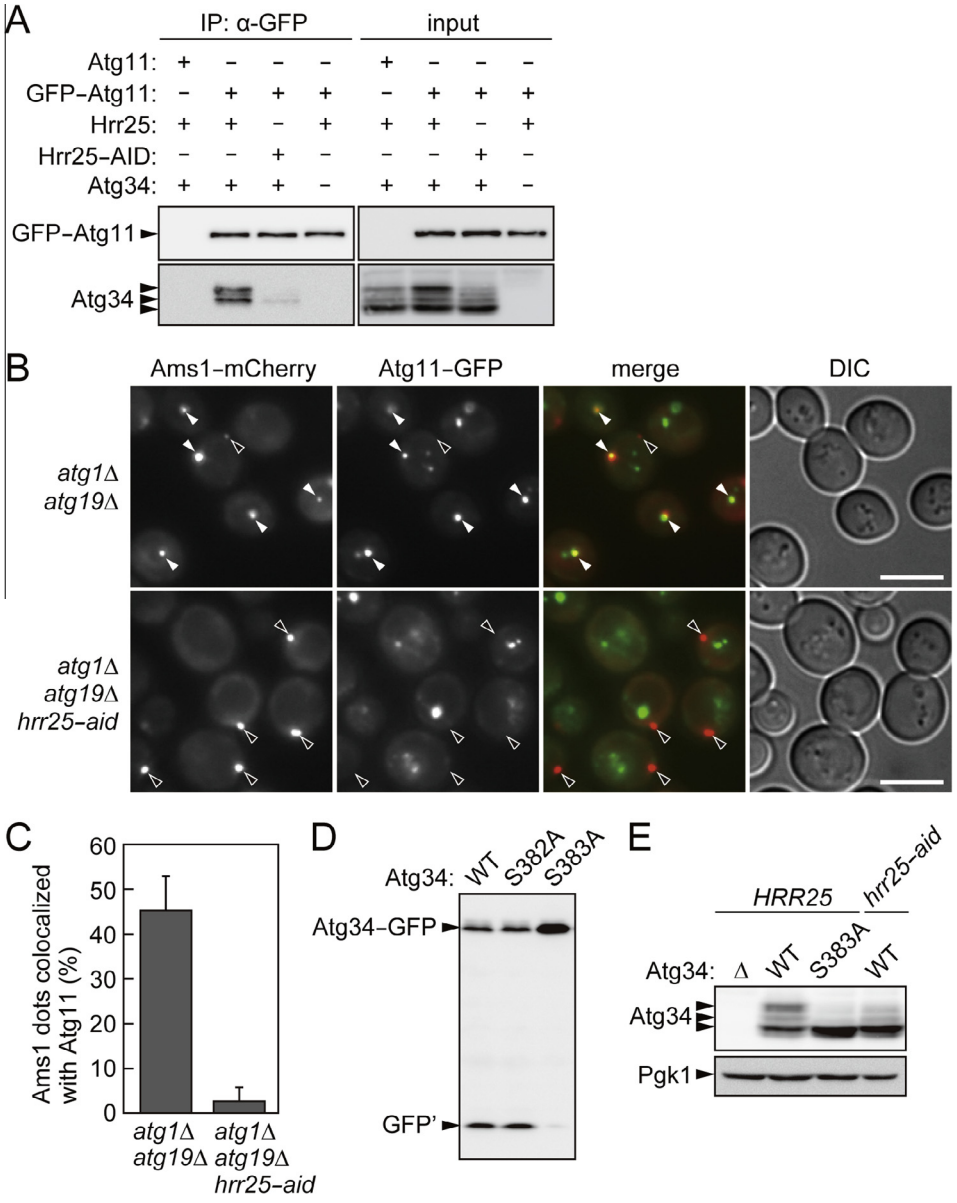

Fig. 4. The Atg34–Atg11 interaction is impaired by Hrr25 depletion. (A) *atg19Δ pep4Δ* cells expressing GFP–Atg11 from the *ADH1* promoter were treated with rapamycin in the presence of IAA for 1 h. The cleavable crosslinking reagent DSP was added to these cells to fix protein–protein interactions. Immunoprecipitation was performed using anti-GFP antibody, followed by immunoblotting using antibodies against GFP and Atg34. (B) The colocalization of Ams1–mCherry and Atg11–GFP was examined as described in Fig. 3B. The white and black arrowheads indicate Ams1–mCherry dots colocalized or not colocalized with Atg11–GFP, respectively. Scale bars, 5 μm. (C) In the experiments shown in (B), Ams1 dots colocalized with Atg11 were counted, and their percentages (%) relative to the total numbers of Ams1 dots are shown with standard deviations ($n = 3$). (D) Cells expressing Atg34–GFP were treated with rapamycin for 6 h in the presence of IAA, and subjected to immunoblotting using antibody against GFP. (E) Phosphorylation of the S383A mutant of Atg34 in cells treated with rapamycin for 6 h was examined as described in Fig. 1D.

with rapamycin, and this Ams1–GFP transport depended on Atg34 (Fig. 2A). *atg19Δ hrr25–aid* cells exhibited a significant defect in vacuolar transport of Ams1–GFP when treated with IAA, and a milder defect in the absence of IAA treatment. Because *hrr25–aid* cells had a slight growth defect even in the absence of IAA, it is likely that addition of the AID tag affected the function of Hrr25 to some degree. Atg34 itself, in association with Ams1, is also delivered into the vacuole [9]. We examined the vacuolar cleavage of Atg34–GFP and showed that knockdown of Hrr25 also decreased Atg34 transport to the vacuole (Fig. 2B). These results suggest that Hrr25-mediated phosphorylation is important for the function of Atg34 in vacuolar transport of Ams1 under nitrogen-starvation conditions.

3.3. Hrr25 promotes Atg11 targeting to the Ams1 complex by enhancing the Atg34–Atg11 interaction

We next asked what function of Atg34 requires Hrr25. During the autophagic transport of Ams1, Atg34 first interacts with Ams1 oligomers to form a higher order assembly called the Ams1 complex, which is observed as dots in fluorescence microscopy of yeast cells expressing Ams1–GFP [6,9]. Hrr25 knockdown affected neither formation of Ams1–GFP dots (Fig. 3A) nor the colocalization of Ams1–mCherry and Atg34–GFP (Fig. 3B). In addition, immunoprecipitation analysis showed that Atg34–GFP coprecipitated with Ams1 in Hrr25-depleted cells to a similar extent to in control cells (Fig. 3C). These results suggested that the function

of Atg34 in the assembly of the Ams1 complex was normal even when Hrr25 was depleted. In the subsequent step, Atg34 recruits the adaptor Atg11 to the Ams1 complex via a direct interaction. Therefore, we examined the impact of Hrr25 depletion on the Atg34–Atg11 interaction. Depletion of Hrr25 substantially diminished the level of Atg34 that coprecipitated with GFP–Atg11 in immunoprecipitation analysis (Fig. 4A). Consistent with this, the colocalization of Atg11–GFP with Ams1–mCherry was severely reduced by Hrr25 depletion (Fig. 4B and C). These results suggest that Hrr25 is required for the interaction of Atg34 with Atg11, i.e., the function of Atg34 in Atg11 recruitment to the Ams1 complex. In immunoprecipitation experiments, phosphorylated forms of Atg34 coprecipitated with Atg11 more efficiently than the unphosphorylated form (Fig. 4A), consistent with the notion that Hrr25-mediated phosphorylation of Atg34 promotes its interaction with Atg11.

A recent study identified two phosphorylated residues (Ser382 and Ser383) in the Atg11-binding region of Atg34 by mass spectrometry, and also reported that the simultaneous Ala replacement of these residues abolished autophagic transport of Ams1 [27]. In this study, we showed that the S383A mutation but not the S382A mutation impaired Atg34 transport to the vacuole (Fig. 4D). We also showed that Hrr25-dependent phosphorylation of Atg34 was not observed in the S383A mutant (Fig. 4E). These results suggest that phosphorylation of Ser383 by Hrr25 is important for Atg34-mediated vacuolar transport of Ams1.

In this study, we showed that Hrr25 phosphorylates Atg34 to upregulate Ams1 transport to the vacuole when cells are starved for nitrogen. What is the physiological significance of this mechanism? Under nutrient-rich conditions, Ams1 functions in the cytoplasm to process free oligosaccharides, which arise by deglycosylation of misfolded proteins retrotranslocated from the ER [28]. However, substantial amounts of these saccharides are likely to be transported into the vacuole by non-selective autophagy under starvation conditions. In addition, almost all autophagosomes contain fragments of the ER, in which oligosaccharides are synthesized [29]. Thus, the demand for Ams1 in the vacuole should increase under starvation conditions. Hrr25-mediated phosphorylation of Atg34 may be a mechanism that coordinates the vacuolar transport of Ams1 with non-selective autophagy in order to meet this metabolic demand.

The data presented here suggest that Hrr25-mediated phosphorylation of Atg34 promotes the Atg34–Atg11 interaction. In parallel with this study, we found that Hrr25 also phosphorylates Ser391 of Atg19, which corresponds to Ser383 of Atg34, to enhance the Atg19-Atg11 interaction, resulting in the stimulation of the Cvt pathway [17]. Similar results were also reported by another group [27]. In addition, we showed that Atg36, a receptor for autophagic degradation of peroxisomes (pexophagy) [30,31], is also phosphorylated by Hrr25 to interact with the common adaptor Atg11 [17]. Moreover, recent studies elucidated that phosphorylation of the specific receptor Atg32 by casein kinase 2 increases its binding to Atg11 to trigger selective autophagy of mitochondria (mitophagy) [31–34]. Thus, it has now been revealed that all the four receptor-mediated selective autophagy pathways in *S. cerevisiae* are regulated by a uniform mechanism: the enhancement of the receptor–adaptor interaction by receptor phosphorylation. It is also the interesting fact that Hrr25 is involved in the regulation of three of the four pathways: Ams1 transport, the Cvt pathway, and pexophagy. These three pathways are promoted under similar conditions, including growth-saturating and nitrogen-deprived conditions [17,30]. A common signal generated under these conditions may stimulate Hrr25 to phosphorylate the three receptors. Future studies should aim to elucidate how receptor phosphorylation by Hrr25 is triggered under these conditions.

Acknowledgements

We thank the members of our laboratory for materials, discussions, and technical and secretarial support; Dr. Kuninori Suzuki for providing yeast strains; and Dr. Nobuo Noda for providing the plasmid pGEX-6P-Atg34. Materials for the AID system were provided by the National Bio-Resource Project (NBRP) of the MEXT, Japan. This work was supported in part by the Funding Program for Next Generation World-Leading Researchers HO220017 (to H.N.) and Grants-in-Aid for Scientific Research 25111003 (to H.N.), 25711005 (to H.N.), and 23000015 (to Y.O.) from the Ministry of Education, Culture, Sports, Science, and Technology of Japan.

References

[1] Nakatogawa, H., Suzuki, K., Kamada, Y. and Ohsumi, Y. (2009) Dynamics and diversity in autophagy mechanisms: lessons from yeast. Nat. Rev. Mol. Cell Biol. 10, 458–467.
[2] Yang, Z. and Klionsky, D.J. (2010) Eaten alive: a history of macroautophagy. Nat. Cell Biol. 12, 814–822.
[3] Mizushima, N., Yoshimori, T. and Ohsumi, Y. (2011) The role of Atg proteins in autophagosome formation. Annu. Rev. Cell Dev. Biol. 27, 107–132.
[4] Kim, J., Scott, S.V., Oda, M.N. and Klionsky, D.J. (1997) Transport of a large oligomeric protein by the cytoplasm to vacuole protein targeting pathway. J. Cell Biol. 137, 609–618.
[5] Scott, S.V., Guan, J., Hutchins, M.U., Kim, J. and Klionsky, D.J. (2001) Cvt19 is a receptor for the cytoplasm-to-vacuole targeting pathway. Mol. Cell 7, 1131–1141.
[6] Hutchins, M.U. and Klionsky, D.J. (2001) Vacuolar localization of oligomeric alpha-mannosidase requires the cytoplasm to vacuole targeting and autophagy pathway components in *Saccharomyces cerevisiae*. J. Biol. Chem. 276, 20491–20498.
[7] Shintani, T., Huang, W.P., Stromhaug, P.E. and Klionsky, D.J. (2002) Mechanism of cargo selection in the cytoplasm to vacuole targeting pathway. Dev. Cell 3, 825–837.
[8] Yuga, M., Gomi, K., Klionsky, D.J. and Shintani, T. (2011) Aspartyl aminopeptidase is imported from the cytoplasm to the vacuole by selective autophagy in *Saccharomyces cerevisiae*. J. Biol. Chem. 286, 13704–13713.
[9] Suzuki, K., Kondo, C., Morimoto, M. and Ohsumi, Y. (2010) Selective transport of alpha-mannosidase by autophagic pathways: identification of a novel receptor, Atg34p. J. Biol. Chem. 285, 30019–30025.
[10] Watanabe, Y., Noda, N.N., Kumeta, H., Suzuki, K., Ohsumi, Y. and Inagaki, F. (2010) Selective transport of alpha-mannosidase by autophagic pathways: structural basis for cargo recognition by Atg19 and Atg34. J. Biol. Chem. 285, 30026–30033.
[11] Janke, C. et al. (2004) A versatile toolbox for PCR-based tagging of yeast genes: new fluorescent proteins, more markers and promoter substitution cassettes. Yeast 21, 947–962.
[12] Nakatogawa, H., Ishii, J., Asai, E. and Ohsumi, Y. (2012) Atg4 recycles inappropriately lipidated Atg8 to promote autophagosome biogenesis. Autophagy 8, 177–186.
[13] Nishimura, K., Fukagawa, T., Takisawa, H., Kakimoto, T. and Kanemaki, M. (2009) An auxin-based degron system for the rapid depletion of proteins in non plant cells. Nat. Methods 6, 917–922.
[14] Sung, M.K. and Huh, W.K. (2007) Bimolecular fluorescence complementation analysis system for in vivo detection of protein–protein interaction in *Saccharomyces cerevisiae*. Yeast 24, 767–775.
[15] Nakatogawa, H. and Ohsumi, Y. (2012) SDS–PAGE techniques to study ubiquitin-like conjugation systems in yeast autophagy. Methods Mol. Biol. 832, 519–529.
[16] Yoshihisa, T. and Anraku, Y. (1990) A novel pathway of import of alpha-mannosidase, a marker enzyme of vacuolar membrane, in *Saccharomyces cerevisiae*. J. Biol. Chem. 265, 22418–22425.
[17] Tanaka, C., et al., Hrr25 triggers selective autophagy-related pathways by phosphorylating receptor proteins. J. Cell Biol. (in press).
[18] Nakatogawa, H., Ichimura, Y. and Ohsumi, Y. (2007) Atg8, a ubiquitin-like protein required for autophagosome formation, mediates membrane tethering and hemifusion. Cell 130, 165–178.
[19] Breitkreutz, A. et al. (2012) A global protein kinase and phosphatase interaction network in yeast. Science 328, 1043–1046.
[20] Hoekstra, M.F., Liskay, R.M., Ou, A.C., DeMaggio, A.J., Burbee, D.G. and Heffron, F. (1991) HRR25, a putative protein kinase from budding yeast: association with repair of damaged DNA. Science 253, 1031–1034.
[21] DeMaggio, A.J., Lindberg, R.A., Hunter, T. and Hoekstra, M.F. (1992) The budding yeast HRR25 gene product is a casein kinase I isoform. Proc. Natl. Acad. Sci. U.S.A. 89, 7008–7012.
[22] Petronczki, M. et al. (2006) Monopolar attachment of sister kinetochores at meiosis I requires casein kinase 1. Cell 126, 1049–1064.
[23] Schafer, T., Maco, B., Petfalski, E., Tollervey, D., Bottcher, B., Aebi, U. and Hurt, E. (2006) Hrr25-dependent phosphorylation state regulates organization of the pre-40S subunit. Nature 441, 651–655.

[24] Lord, C., Bhandari, D., Menon, S., Ghassemian, M., Nycz, D., Hay, J., Ghosh, P. and Ferro-Novick, S. (2011) Sequential interactions with Sec23 control the direction of vesicle traffic. Nature 473, 181–186.
[25] Noda, T. and Ohsumi, Y. (1998) Tor, a phosphatidylinositol kinase homologue, controls autophagy in yeast. J. Biol. Chem. 273, 3963–3966.
[26] Murakami, A., Kimura, K. and Nakano, A. (1999) The inactive form of a yeast casein kinase I suppresses the secretory defect of the sec12 mutant. Implication of negative regulation by the Hrr25 kinase in the vesicle budding from the endoplasmic reticulum. J. Biol. Chem. 274, 3804–3810.
[27] Pfaffenwimmer, T. et al. (2014) Hrr25 kinase promotes selective autophagy by phosphorylating the cargo receptor Atg19. EMBO Rep. 15, 862–870.
[28] Hirayama, H., Seino, J., Kitajima, T., Jigami, Y. and Suzuki, T. (2010) Free oligosaccharides to monitor glycoprotein endoplasmic reticulum-associated degradation in *Saccharomyces cerevisiae*. J. Biol. Chem. 285, 12390–12404.
[29] Hamasaki, M., Noda, T., Baba, M. and Ohsumi, Y. (2005) Starvation triggers the delivery of the endoplasmic reticulum to the vacuole via autophagy in yeast. Traffic 6, 56–65.
[30] Motley, A.M., Nuttall, J.M. and Hettema, E.H. (2012) Pex3-anchored Atg36 tags peroxisomes for degradation in *Saccharomyces cerevisiae*. EMBO J. 31, 2852–2868.
[31] Farre, J.C., Burkenroad, A., Burnett, S.F. and Subramani, S. (2013) Phosphorylation of mitophagy and pexophagy receptors coordinates their interaction with Atg8 and Atg11. EMBO Rep. 14, 441–449.
[32] Kanki, T., Wang, K., Cao, Y., Baba, M. and Klionsky, D.J. (2009) Atg32 is a mitochondrial protein that confers selectivity during mitophagy. Dev. Cell 17, 98–109.
[33] Okamoto, K., Kondo-Okamoto, N. and Ohsumi, Y. (2009) Mitochondria-anchored receptor Atg32 mediates degradation of mitochondria via selective autophagy. Dev. Cell 17, 87–97.
[34] Kanki, T. et al. (2013) Casein kinase 2 is essential for mitophagy. EMBO Rep. 14, 788–794.
[35] Darsow, T., Rieder, S.E. and Emr, S.D. (1997) A multispecificity syntaxin homologue, Vam3p, essential for autophagic and biosynthetic protein transport to the vacuole. J. Cell Biol. 138, 517–529.